Environmental Science & Technology

Article

Cite This: Environ. Sci. Technol. 2018, 52, 2658−2667

pubs.acs.org/est

# Phosphorus Speciation and Solubility in Aeolian Dust Deposited in the Interior American West

Zhuojun Zhang,[†,∥,⊥] Harland L. Goldstein,[‡] Richard L. Reynolds,[‡] Yongfeng Hu,[§] Xiaoming Wang,[†] and Mengqiang Zhu*[,†]

[†]Department of Ecosystem Science and Management, University of Wyoming, Laramie, Wyoming 82071, United States

[‡]Geosciences and Environmental Change Science Center, U.S. Geological Survey, Denver, Colorado 80225, United States

[§]Canadian Light Source Incorporated, University of Saskatchewan, Saskatoon, Saskatchewan S7N 2V3, Canada

[∥]State Key Laboratory of Environmental Geochemistry, Institute of Geochemistry, Chinese Academy of Sciences, Guiyang 550081, China

[⊥]University of Chinese Academy of Sciences, Beijing 100049, China

Supporting Information

**ABSTRACT:** Aeolian dust is a significant source of phosphorus (P) to alpine oligotrophic lakes, but P speciation in dust and source sediments and its release kinetics to lake water remain unknown. Phosphorus K-edge XANES spectroscopy shows that calcium-bound P (Ca−P) is dominant in 10 of 12 dust samples (41−74%) deposited on snow in the central Rocky Mountains and all 42 source sediment samples (the fine fraction) (68−80%), with a lower proportion in dust probably because acidic snowmelt dissolves some Ca−P in dust before collection. Iron-bound P (Fe−P, ∼54%) dominates in the remaining two dust samples. Chemical extractions (SEDEX) on these samples provide inaccurate results because of unselective extraction of targeted species and artifacts introduced by the extractions. Dust releases increasingly more P in synthetic lake water within 6−72 h thanks to dissolution of Ca−P, but dust release of P declines afterward due to back adsorption of P onto Fe oxides present in the dust. The back sorption is stronger for the dust with a lower degree of P saturation determined by oxalate extraction. This work suggests that P speciation, poorly crystalline minerals in the dust, and lake acidification all affect the availability and fate of dust-borne P in lakes.

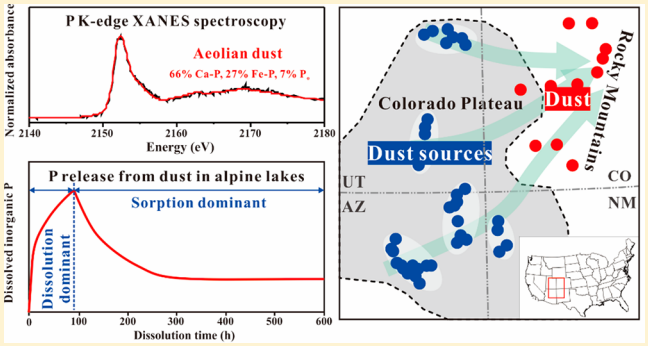


## INTRODUCTION

Phosphorus (P) can limit the primary productivity of oligotrophic alpine lakes due to the low P input from poorly weathered surrounding watersheds.[1,2] In such environments, mineral dust derived from dryland sediments is potentially an important P source, in particular when referring to alpine lakes[3−10] located at the margins of continental arid and semiarid regions, where dust mobilization and deposition are massive.[11] The P supply from dust deposition can alter the nutrient-limitation regime,[3,8,12,13] stimulate primary productivity, and shift bacterial abundance and phytoplankton-species composition[14−16] in most alpine lacustrine ecosystems.

Not all forms of P carried by dust are available in aquatic ecosystems. The availability, fate, and behavior of dust-borne P in alpine lakes can be affected by both P speciation and water chemistry. Sequential extractions were used to characterize speciation of dust-borne P and have improved the understanding of its bioavailability.[17−19] However, the extraction-derived P pools are operational and do not necessarily correspond to P species.[20,21] Phosphorus K-edge X-ray absorption near edge structure (XANES) spectroscopy provides more detailed and precise information on P speciation.[22−27] XANES spectroscopy divides solid P into P bound to Ca (Ca−P), Fe (Fe−P), Al (Al−P), and organic matter ($P_o$).[22] To date, only two studies reported P XANES analysis of the speciation of dust-borne P.[28,29] Main results of these works showed that European anthropogenic aerosols are rich in $P_o$, polyphosphate, and alkali phosphate,[28] whereas P speciation in Saharan dust collected at dust-emission sites is dominated by Ca−P and Fe−P.[28,29] The dust samples in these studies were enriched in anthropogenic aerosols[28] or collected at dust emission sites.[29] The results may be inapplicable to mineral dust received in downwind continental terrestrial ecosystems because the speciation of dust-borne P is related to dust source regions and travel distances. Dust collected at

Received: September 13, 2017
Revised: February 6, 2018
Accepted: February 8, 2018
Published: February 8, 2018






DOI: 10.1021/acs.est.7b04729
Environ. Sci. Technol. 2018, 52, 2658−2667

source sites may not represent that at deposition sites because internal mixing with other sources[28,30] and atmospheric processing[31,32] during dust transport prior to collection could cause P transformation.

Physicochemical factors, such as pH, of the ecosystems where aeolian dust is deposited, strongly affect P behavior after deposition. Only 15−30% of P is water-soluble in aerosol samples reaching the Gulf of Aqaba[18] because of the alkaline seawater (pH ≈ 8.2), whereas Saharan dust can be weathered intensively upon arrival and release most of the P in the Amazon basin[33] due to its highly acidic soils (pH 4.17−4.94).[34] In addition to the amount of P released, the kinetics of P release are important as they affect temporal availability of dust-borne P. Previous dissolution kinetic experiments showed that dust released increasingly more dissolved inorganic P (DIP) to seawater over time.[35,36] In contrast, an initial increase followed by a decline in DIP was observed during dust-seeding experiments in seawater.[37] The decline was ascribed to P adsorption back onto mineral particles in the dust.[37] However, the kinetics of P release from dust in fresh alpine lake water remain unknown,[3−10] and they may differ from those observed in seawater because of their distinct water chemistry.[38−40]

The semiarid Colorado Plateau region is one of the main dust sources in the western U.S.[41−45] Increased dust emission due to extensive grazing and prolonged aridity in the western U.S. has increased P loading to nearby alpine lakes in the Rocky Mountain area.[6,7,10] The pH of the alpine lakes ranges between pH 4.5 and 7.5 due to different degrees of lake acidification caused by elevated atmospheric nitrogen deposition.[38−40] In the present study, we identified the solid-phase speciation of P in dust collected in the central Rocky Mountains of Colorado and sediment samples from major potential source areas using sequential extractions combined with P K-edge XANES spectroscopy. We further evaluated the accuracy of the extractions by characterizing the P speciation in each pool using XANES spectroscopy to provide insights into the usefulness of this method. To better comprehend the biogeochemical impact of dust-borne P deposition in alpine lacustrine environments, we investigated P release kinetics through the dissolution experiments using synthetic alpine lake water of pH 5.0−7.5.

## MATERIALS AND METHODS

**Sampling and Pretreatment.** Dust samples were collected from snow cover in the central Rocky Mountains of Colorado (Figure 1) during late spring, representing the merged accumulation of all dust layers deposited to snow during water year 2014 (October 1, 2013 to September 30, 2014). Sites were sampled by the Center for Snow and Avalanche Studies for investigation of effects of dust on snowmelt processes and rates. Complete site descriptions can be found at http://www.codos.org/. Samples were sent to the Geosciences and Environmental Change Science Center of the U.S. Geological Survey in Denver, CO, where snow was evaporated at 35 °C. The dried dust samples were preserved at room temperature before analyses.

We collected surface-sediment samples from five high and arid basins: The Uinta Basin, Hanksville area, Chinle Valley, Chuska Valley, and Little Colorado River basin (LCR) (Figure 1). These basins are the major potential source areas of the dust samples on the basis of dust particle sizes, back-trajectory analyses, and direct observation, as discussed in detail in Supporting Information Text SI-1. Surface-sediment samples

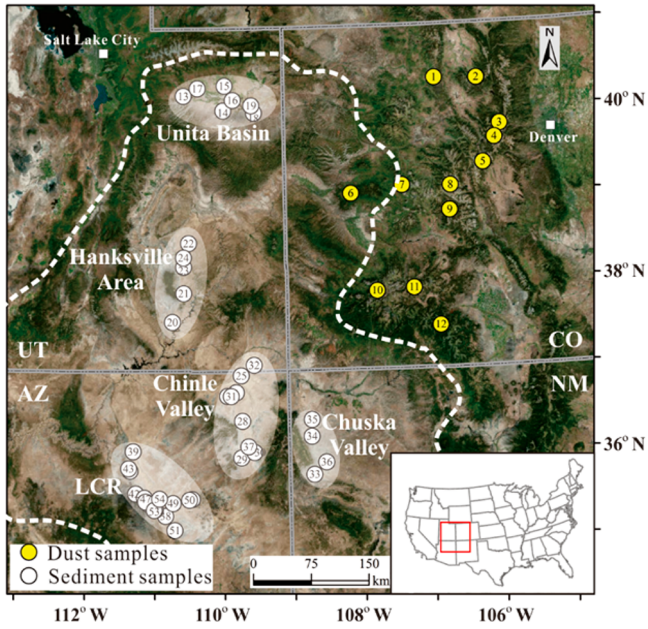


**Figure 1.** A satellite image showing the locations where the dust (yellow circles) and source sediment (white circles) samples were collected (see Table S2 for the coordinates). The dust sampling sites are located in the central Rocky Mountains of Colorado, listed as follows: 1, Rabbit Ears Pass (REP); 2, Willow Creek Pass (WCP); 3, Berthoud Pass (Berth); 4, Grizzly Peak (GrP); 5, Hoosier Pass (HP); 6, Grand Mesa (GM); 7, McClure Pass (McClP); 8, Independence Pass (IndP); 9, Park Cone (PC); 10, Swamp Angel (SASP); 11, Spring Creek Pass (SCP); and 12, Wolf Creek Pass (WoCrP). The dust source sites are centered in five areas on the Colorado Plateau (white dashed line): the Uinta Basin, Hanksville area, Chinle Valley, Chuska Valley, and Little Colorado River (LCR) basin. Map data from Esri, DigitalGlobe, GeoEye, Earthstar Geographics, CNES/Airbus DS, USDA, USGS, AeroGRID, IGN, and the GIS User Community.

were dried and sieved to obtain the size fraction passing through 63-$\mu$m sieve for the further analysis because the dust contains more than 77% of particles smaller than 63 $\mu$m (Table S1). The mineralogy of the dust samples and two surface samples was determined by X-ray diffraction (XRD; Table S-2). Poorly and well-crystallized Al and Fe ($Fe_{ox}$, $Fe_d$, $Al_{ox}$) were quantified using oxalate and dithionite extractions, respectively.[46] See the details of all samples in Table S2.

**Sequential Chemical Extractions.** The operationally defined P pools in the dust and source sediments were determined using the sequential extraction method (SEDEX)[47,48] that was developed for aquatic sediments. This method was selected for dust[17−19,29] because dust deposited to aquatic ecosystems is incorporated into aquatic sediments eventually. This method allowed for quantification of five major operationally defined P pools: (i) water-soluble P, (ii) exchangeable and reactive Fe-bound P (CDB-P, extracted with a citrate-dithionite-bicarbonate solution), (iii) authigenic apatite P (Acet-P, extracted with acetic acid-sodium acetate), (iv) detrital P (Det-P, extracted with 1 M HCl without ashing), and (v) organic P ($P_o$). Detailed procedures are provided in SI-2. The P concentration in each extract was determined using the standard molybdate blue method[49] except for the CDB-P because the composition of the CDB extracts interferes with the molybdate blue method. The CDB-P was measured using inductively coupled plasma atomic emission spectroscopy. Four dust samples (others did not have enough mass) and all


DOI: 10.1021/acs.est.7b04729
Environ. Sci. Technol. 2018, 52, 2658−2667

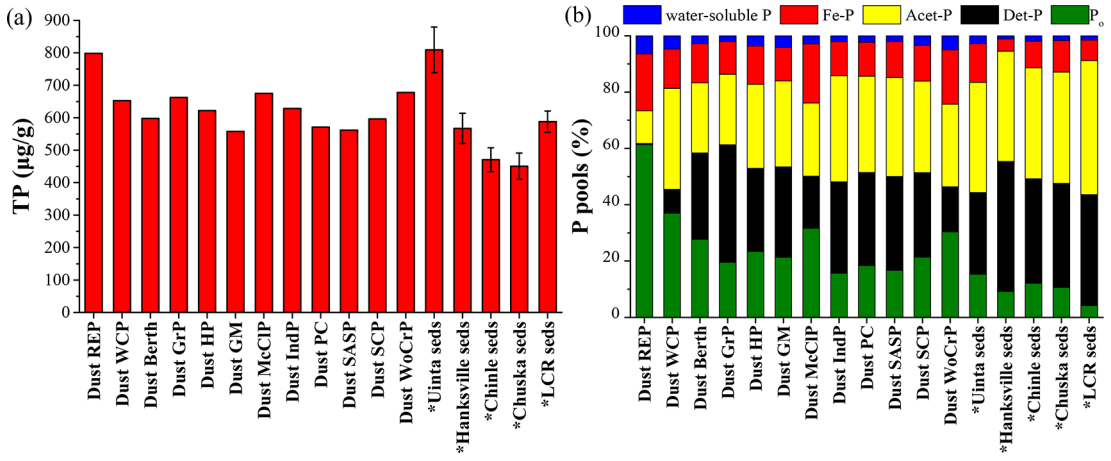


**Figure 2.** (a) The total P concentrations in dust and sediment samples; (b) the relative fraction of each P pool in dust and sediment samples as determined by SEDEX. The mean RSD for both TP and each pool is 6.5%, based on duplicate analyses. *TP in the source sediments are represented by means ± standard errors. Standard errors for water-soluble P, Fe−P, Acet-P, Det-P, and $P_o$ in sediments are 0.5%, 2.4%, 4.5%, 7.8%, and 3.3%, respectively.

sediment samples were analyzed in duplicate to assess the reproducibility of the extractions. See SI-2 for more details.

**Phosphorus K-Edge XANES Spectroscopy.** The spectra were collected from both the dust and the source sediment samples at room temperature at the Soft X-ray Micro-Characterization Beamline (SXRMB) at the Canadian Light Source, Saskatoon, Canada. The spectra were background removed, normalized, and then subject to linear combination fitting (LCF) analysis to determine P speciation. A set of P reference compounds were used for spectral fitting, including well-crystallized and poorly crystalline hydroxyl apatite (Ca−P), phosphate adsorbed on ferrihydrite and goethite (Fe−P), phosphate adsorbed on kaolinite (Al−P), and phytate ($P_o$). The preparation procedures of the references are provided in SI-3. Four or fewer reference spectra were used in the LCF for each sample. Energy was not allowed to float during the fitting. The combination of the Ca−P, Fe−P, and $P_o$ reference spectra yielded the best fits for all samples.

To validate the operational definitions of P pools obtained by SEDEX, we characterized the speciation of P in each pool for three selected dust samples (REP, GM, and SASP) using XANES spectroscopy. The P XANES spectra of solid residues after each extraction step were measured, and the difference spectra were obtained by subtracting the spectra of the successive steps.[20] The difference spectra were analyzed with the LCF analysis to determine the P speciation of each pool.

**Phosphorus Release Kinetics.** The experiment was performed on the dust samples using synthetic lake water (SLW) of different pHs. Four representative dust samples (REP, GM, McClP, and SASP) were selected based on the XANES-derived P speciation. SLW was made based on the reported major ion composition (50 μM $CaCO_3$, 20 μM $NaHCO_3$, 10 μM $MgSO_4$, 3 μM $KNO_3$, 2 μM KCl, and 1 μM $NH_4Cl$) and pH (5, 6.5, and 7.5) of the alpine lake water in the Rocky Mountains of Colorado.[38−40] The solution was agitated for 3 days to ensure the chemicals were dissolved completely. Then the pH was maintained at the target value by adding 0.1 M HCl for 1 day before use for the release experiments, and the pH changed negligibly during the entire period of experiments. Eighty mg dust was added to an acid-washed plastic bottle (Nalgene) containing 1000 mL SLW. The bottle was agitated in a shaker at room temperature. Aliquots were taken at <10 min (t0), 6 h (t6), 1 d (t24), 3 d (t72), 7 d (t168), 14 d (t336), and 24 d (t576). For sampling, the bottle was vigorously stirred on a magnetic stirring plate to homogenize the suspension, and an aliquot of 140 mL suspension was removed and filtered through 0.2 μm polypropylene syringe filters for DIP analysis. The control experiments (no dust addition) were conducted using the identical procedure in the absence of dust.

Because the solution samples contained an ultra-low level of DIP, a modified magnesium (Mg) hydroxide co-precipitation method MAGIC[50] was used to determine the DIP concentrations. Here, we used high-purity Mg standard in 2% nitric acid matrix (Inorganic Ventures, 10 000 μg/mL) as the P-free Mg source. About 1 mM (millimoles per liter) Mg solution was used, achieving slight supersaturation with respect to $Mg(OH)_2$ pellets, and contributing a negligible amount of DIP (0.0047 nanomole per liter). In brief, 1 mL 45 mM Mg standard solution was added into 40 mL sample, followed by addition of 0.2 mL 1 M NaOH, capping and shaking, and sitting for 20 min at room temperature. Then, the precipitate was collected by centrifugation of 5 min at 2700*g*. After dissolution of the precipitate in 0.8 mL 1 M HCl, the solution was analyzed using the standard molybdate blue method.[49] All chemicals used in these experiments were of trace metal grade. Due to the limited mass, only the release experiment with dust SASP at pH 6.5 was repeated to examine the reproducibility of the kinetic experiments. The detection limit of DIP was 0.01 μM ($n$ = 6) based on three times the standard deviation of the blanks.

## RESULTS AND DISCUSSION

The total P (TP) concentration is 562−798 μg/g in the dust and 809 ± 70, 567 ± 46, 471 ± 37, 451 ± 41, and 588 ± 33 μg/g (mean ± standard error) in the Uinta, Hanksville, Chinle, Chuska, and LCR source sediments (<63 μm) (Figure 2a, Table S3), respectively. Mineralogy, as well as concentrations of extracted Fe and Al are listed in Table S2.

**Phosphorus Speciation.** The P K-edge XANES spectra of all dust samples except for REP and GM exhibit a strong shoulder peak at 2155 eV and two post-edge peaks at 2163 and 2169 eV as well (Figure 3b). These spectral features are similar to those of apatite (Figure 3a), indicating dominance of Ca−P. The post-edge spectral features of REP and GM are not as clearly resolved as the dust samples at other sites, but the


DOI: 10.1021/acs.est.7b04729
Environ. Sci. Technol. 2018, 52, 2658−2667

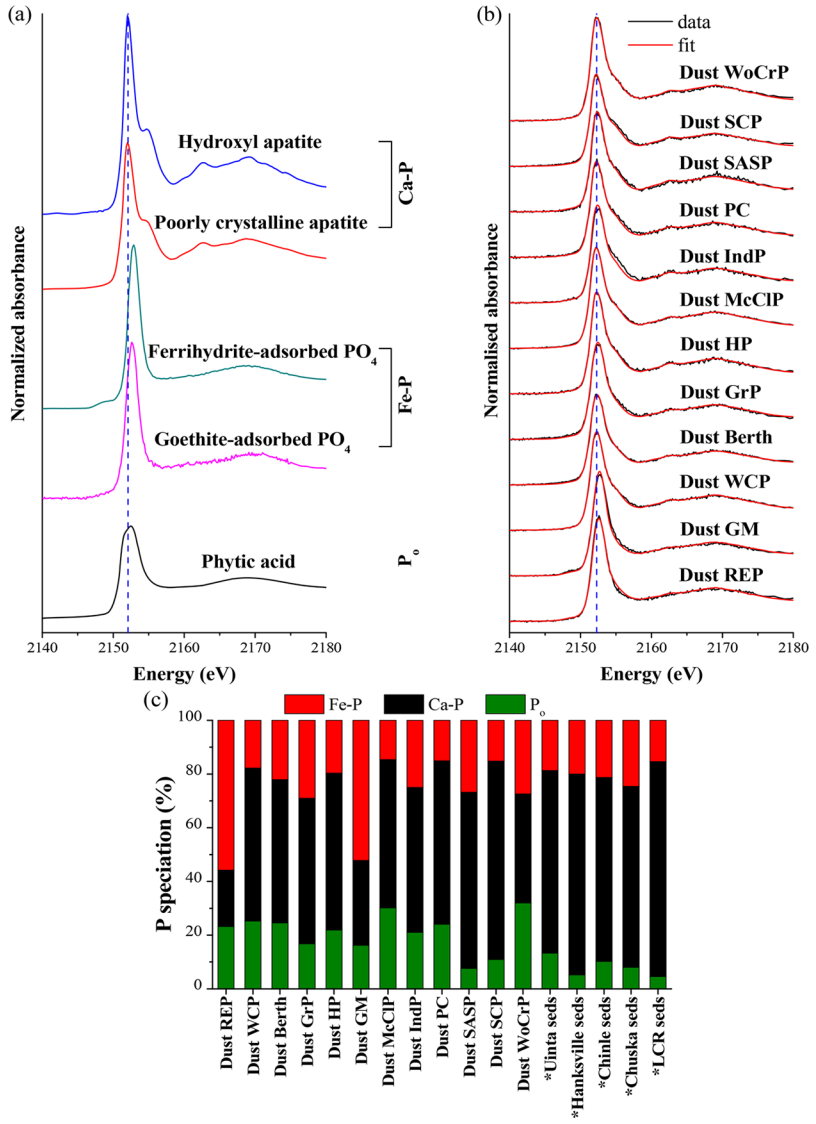


**Figure 3.** (a) Phosphorus K-edge XANES spectra of the reference compounds, including hydroxyl apatite and poorly crystalline apatite representing Ca−P, ferrihydrite-, and goethite-adsorbed $PO_4$ representing Fe−P, and phytic acid representing organic P; (b), the linear combination fits (LCF) of the P spectra for the dust samples; and (c) the relative fractions of each P species in dust and sediment samples as determined by the LCF analysis. *The source sediments are represented by mean values at each site. The mean relative standard deviation (RSD) of the XANES fitting is 5%.

spectra have the pre-edge peaks at 2150 eV, and their white-lines shift to higher energy relative to apatite. These are the characteristic features of Fe−P, indicating an important fraction of Fe−P in REP and GM (Figure 3a, b). Consistently, the LCF results indicate that REP and GM contain 52.2−55.8% Fe−P, 21−31.6% Ca−P, and 16.2−23.2% $P_o$. The remaining 10 dust samples contain 40.6−73.9% (mean 57.3%) Ca−P, 14.6−29% Fe−P (mean 21.3%), and 7.6−32% (mean 21.4%) $P_o$ (Figure 3c, Table S3). Previous P K-edge XANES results show that dust originating from the Saharan desert soils contains 25−95% Ca−P and 28−60% Fe−P.[28,29]

The XANES spectra of all sediment samples in the five source areas closely resemble the apatite spectra, indicating the dominance of Ca−P (Figure S5). The LCF results show that the sediments contain mean values of 68−80% Ca−P, 15.4−24.6% Fe−P, and 4.6−13.3% $P_o$. The P speciation is consistent with the alkaline sediments and the presence of calcareous sedimentary rock formations on the Colorado Plateau.[51,52]

The dust samples contain lower portions of Ca−P and higher portions of both $P_o$ and Fe−P than the source sediments. The comparison result is the same after excluding $P_o$ from the dust (Figure S6a); hence the accumulation of high levels of $P_o$ in the dust is not the sole reason for the lower Ca−P fractions in the dust. The difference between the dust and sediments is ascribed to other unknown P sources of dust or atmospheric and snowmelt processing that alters P speciation in the dust before dust collection.

Atmospheric acidification during dust transport can dissolve apatite, particularly in offshore areas of oceans where mineral aerosols interact with air masses polluted by anthropogenic $SO_2$ and $NO_x$.[31,32] However, in the present study, the dust travels much shorter distances (hundreds of kilometers) across the dry continental region,[6] not allowing for significant alteration of P speciation. Instead, acid processing of dust more likely occurs during weeks- or months-long snow melting as the snowmelt is acidic in the Rocky Mountain regions and can dissolve carbonates[51,53] and other alkaline materials (e.g., apatite).



DOI: 10.1021/acs.est.7b04729
Environ. Sci. Technol. 2018, 52, 2658−2667

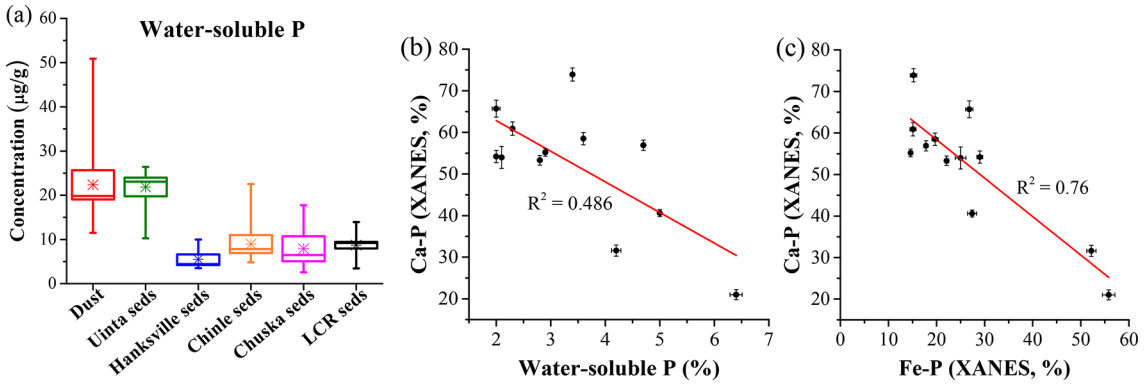


**Figure 4.** (a) Water-soluble P concentrations of the dust and sediment samples. The upper and lower edges of the boxes depict mean ± standard errors, the center lines in the boxes indicate the median values, and the asterisks denote the mean values. The lines show the range of the value. The sample size for the statistical analysis is 12, 7, 5, 8, 5, and 17 for dust, Uinta, Hanksville, Chinle, Chuska, and LCR sediments, respectively. A plot of XANES-derived Ca−P fraction versus water-soluble P (b), and the XANES-derived Fe−P fractions (c) for the dust samples. The error bars shown in b and c indicate the standard errors of measurements. Eight of the dust samples were not measured for multiple times to determine error bars for water-soluble P because of their limited sample mass. The red lines represent linear regressions.

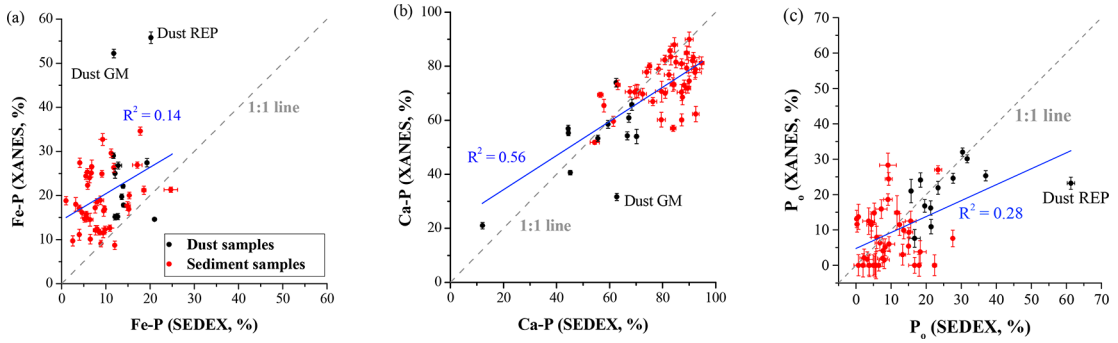


**Figure 5.** Comparison of Fe−P (a), Ca−P (b), and organic P (c) as determined by SEDEX and P K-edge XANES spectroscopy for all dust and sediment samples. The SEDEX-determined Ca−P is the sum of the authigenic and detrital P. The gray dashed lines show the 1:1 relationship. The linear regression (blue lines) is based on all the data points. The data points corresponding to dust REP and GM are labeled as they deviate the most from the 1:1 line among all dust samples.

The dissolution of apatite might increase the water-soluble P of dust (Figure 4a), indicated by a negative correlation between the water-soluble P and Ca−P (Figure 4b). Calcium can also be leached out of dust, resulting in the lower Ca contents in the dust than in the sediments (Table S3). Given that the dust contains abundant Fe oxides (Table S2), P released by snowmelt acidification may react with Fe oxides within the dust particles, forming additional Fe−P and hence increasing the Fe−P fractions in the dust (Figures 3c and S6a), which is consistent with a strong negative correlation between the Ca−P and Fe−P fractions (Figure 4c).

The rearrangement of P speciation within dust caused by acidification in snowmelt could contribute to the exceptionally high Fe−P fractions (>50%) in REP and GM if the snowmelt at the two sites are highly acidic. However, the exceptionally high levels of Fe−P are also likely caused by input of other dust sources containing abundant Fe−P. For example, wood ash, produced from biomass burning, is rich in Fe−P (~68%)[18] and may incorporate into REP and GM.

The higher levels of $P_o$ in dust than in the sediments probably result from mixing with diverse organic materials during transportation and deposition of mineral dust prior to collection, including wildfire ash, pollen, microorganisms, and other forms of windblown plant materials.[28,41,54,55] The different $P_o$ concentration among the dust samples suggests varying amounts of $P_o$ input to the dust at different sampling sites.

Additionally, P speciation may be related to the local topography of the sites. Dust deposited at high-elevation sites tends to contain less $P_o$ than those at low-elevation sites (Figure S7a), which is likely attributed to the greater amount of biomass at low-elevation sites.[56] Meanwhile, relatively less Ca−P with respect to the low-elevation sites (Figure S7c) occurs probably because the acid processing in snowmelt is enhanced by high temperature and increased availability of snowmelt at low elevation. In summary, varying degrees of snowmelt processing, diverse atmospheric pathways, and varying unknown material inputs are responsible for the large variations of P speciation in the dust.

**Operationally Defined P Pools.** The size of each P fraction based on SEDEX varies greatly among the dust samples. The dust-borne P is composed of 11.6−37.7% (mean 29.4%) authigenic P, 0.5−41.7% (mean 25.5%) detrital P, 15.7−61.3% (mean 27.0%) $P_o$, 11.8−21.0% (mean 14.6%) Fe−P, and 2.0−6.4% (mean 3.4%) water-soluble P (Figure 2b, Table S3). Consistent with the XANES analysis, dust deposited at lower elevations contains more $P_o$ and probably less authigenic and detrital P (together as Ca−P) than at higher elevations (Figure S8). Our dust samples contain much less detrital P than the coastal aerosols of eastern Asia (53−92%)[17]



DOI: 10.1021/acs.est.7b04729
Environ. Sci. Technol. 2018, 52, 2658−2667

**Table 1. XANES LCF-Derived Speciation of P in the Whole Dust, and Extracted by CDB (the Fe−P Pool), Acetate (the Authigenic P Pool), and HCl (the Inorganic P) for Dust REP, GM, and SASP[a]**

| | pool | TP[b] (μg/g) | Fe−P% | Ca−P% | $P_o$% | $R^c$ | TFe-P[d]% | TCa-P[d]% | $TP_o$[d]% |
|---|---|---|---|---|---|---|---|---|---|
| REP | whole dust | 798 (8.5) | 55.8 (1.3) | 21.0 (1.2) | 23.2 (1.7) | 0.003 | | | |
| | Fe−P | 212 (1.9) | 77.9 (2.1) | 17.5 (1.8) | 4.6 (2.7) | 0.007 | 37.2 | 22.2 | 5.2 |
| | authigenic P | 92.5 (2.2) | 0.4 (2.1) | 36.1 (1.8) | 63.5 (2.6) | 0.011 | 0.1 | 20.0 | 31.7 |
| | inorganic P | 309 (2.1) | 49.1 (1.6) | 36.2 (1.3) | 14.8 (1.9) | 0.005 | 34.1 | 66.7 | 24.7 |
| GM | whole dust | 558 (1.2) | 52.2 (1.0) | 31.6 (1.3) | 16.2 (2.0) | 0.006 | | | |
| | Fe−P | 89.5 (0) | 69.0 (1.4) | 23.4 (2.1) | 7.6 (2.9) | 0.013 | 21.2 | 11.9 | 7.5 |
| | authigenic P | 170 (1.4) | 22.2 (1.1) | 63.2 (1.5) | 14.6 (2.2) | 0.008 | 13.0 | 61.1 | 27.5 |
| | inorganic P | 439 (0.9) | 55.9 (1.1) | 35.2 (1.6) | 8.9 (2.4) | 0.008 | 84.3 | 87.8 | 43.2 |
| SASP | whole dust | 561 (9) | 26.8 (0.8) | 65.7 (2.0) | 7.6 (2.5) | 0.005 | | | |
| | Fe−P | 83.6 (4.1) | 28.9 (1.8) | 63.4 (4.5) | 7.8 (5.5) | 0.024 | 16.0 | 14.4 | 15.3 |
| | authigenic P | 197 (2.1) | 26.7 (1.7) | 71.1 (4.3) | 2.2 (5.4) | 0.018 | 35.0 | 37.9 | 10.4 |
| | inorganic P | 468 (3.7) | 24.4 (0.9) | 73.0 (2.2) | 2.6 (2.7) | 0.005 | 75.9 | 92.6 | 28.3 |

[a]Standard errors are given in parentheses. [b]Total P. [c]R-factor = $\Sigma i(XANES_{experimental} - XANES_{fit})^2/\Sigma i(XANES_{experimental})^2$. [d]The percentage of the P species in each extractable pool relative to those in the whole dust.

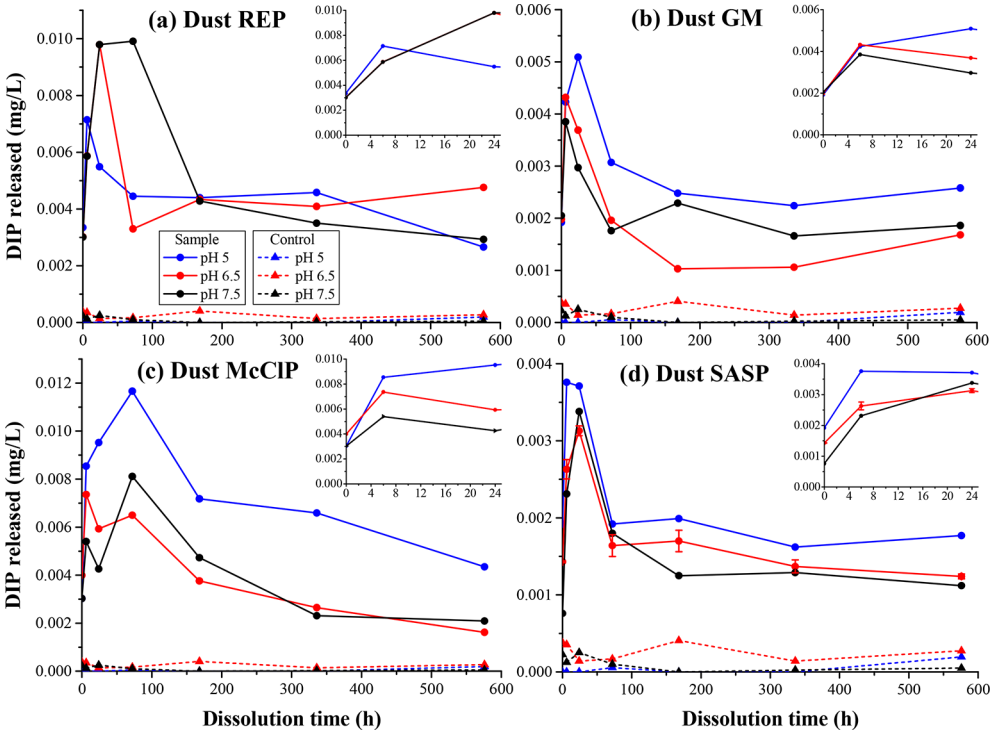


**Figure 6.** Dissolved inorganic P (DIP) released from dust in synthetic lake water at room temperature. Inset: the DIP concentration over the first 24 h of dissolution. (a) REP, (b) GM, (c) McClP, and (d) SASP. The error bars on SASP at pH 6.5 indicate the standard errors from duplicate experiments. The RSD of each time point was estimated to be <14% based on the duplicate experiments with dust SASP (d).

and slightly less authigenic P than the aerosols reaching the Gulf of Aqaba.[18]

The source-area sediments show much lower variations among samples compared to the dust. The apatite P is the dominant form (68.2−86%), consisting of mean 39.1−47.6% authigenic P and 29−46.2% detrital P, whereas Fe−P contributes less than 15%. Organic P only contributes 4−15% of TP. These source sediments (<63 μm) contain similar amounts of apatite as the Saharan soils (fine- to medium-grained sand)[29,31] and sands (<63 μm) from the arid regions of Asia.[57,58]

The dust contains lower proportions of authigenic and detrital P, and higher proportions of water-soluble P and Fe−P than the source sediments (Figures 2b and S6b). Again, the differences can be ascribed to the acid processing in snowmelt (Figure S9), as discussed above. Similarly, aerosol samples above oceans have greater fractions of soluble P than dust-soil precursors or aerosols collected closer to the dust source[17,18,28,59] due to the acid processing during atmospheric transport.

**Comparison of SEDEX and XANES Spectroscopy.** The SEDEX protocol is commonly used for P fractionation in aquatic sediments. However, our results indicate that the operationally defined P fractions are different from the XANES-derived P speciation. The difference is particularly significant for dust samples REP, WCP, and GM (Figures 2b and 3c). Overall, SEDEX underestimates Fe−P for most of the dust and sediment samples, and no correlation exists between the two methods (Figure 5a). Despite some agreements for Ca−P and $P_o$ (Figure 5b, c), most data points deviate significantly from



DOI: 10.1021/acs.est.7b04729
Environ. Sci. Technol. 2018, 52, 2658−2667

the 1:1 relation line and the difference can be up to 40% of TP (Figure S10b, c). Although the uncertainty of the XANES LCF analysis may be as much as 10%,[60] such uncertainty cannot explain the marked difference between XANES and SEDEX results. The discrepancy is more likely due to a lack of specificity in the chemical fractionations.[20,23]

We chose three representative dust samples (REP, GM, and SASP) that differ in P speciation to further characterize the P speciation of each extraction pool (Figure S11). The XANES results show that each pool contains a mixture of P species, and the species most affected by a given extraction is not necessarily the one that is initially assumed to be (Table 1). The form of P removed by the CDB extraction represents the Fe−P pool, but CDB removes only 16% to 37% of total Fe−P (Table 1), probably due to the low efficiency of CDB in dissolving crystalline Fe oxides.[61] The HCl pool is assumed as the total inorganic P in SEDEX, but HCl extracts only 34% - 84% of total Fe−P, and 67−93% of total Ca−P. The incomplete dissolution of the inorganic P species (i.e., Ca−P and Fe−P) by HCl extraction leads to the overestimation of $P_o$ since the $P_o$ pool size is the difference between the total P and the HCl-extracted P.

The P speciation of each pool determined from XANES spectroscopy also suggests that P bound to the same type of metals can have distinct reactivity. The HCl extraction removes only 34% of total Fe−P and 67% of total Ca−P from REP, but 76−84% of total Fe−P and 88−93% of total Ca−P is removed from GM and SASP (Table 1). Thus, the Ca−P and Fe−P in REP are more chemically stable than those in GM and SASP.

In summary, the SEDEX results can be misleading for the dust and sediment samples, and the degree of accuracy depends on the physicochemical properties of the samples that affect extraction efficiencies. In contrast, a good agreement between SEDEX and XANES results is observed for marine sediments,[27] suggesting that SEDEX well assesses speciation of P in aquatic sediments but not in aeolian dust and dryland sediments. The previously reported SEDEX results on aeolian dust[17,18] thus need to be interpreted cautiously.

**Solubility of Dust-Borne P in Synthetic Lake Water.** Under all experimental conditions, the DIP concentration increases within the first 6−72 h and then decreases during the next week. It finally remains constant or declines slightly until the end of the experiments 576 h later (Figure 6).

The decline of the DIP concentration can be attributed to two different processes: biological uptake and/or resorption back to dust particles. Low temperature can suppress microbial growth and metabolism, and accordingly decrease P consumption.[62,63] Thus, we examined the DIP release at 4 °C to test whether biological uptake occurs. We found that the low temperature results in a lower DIP at the late stage, but it does not change the increase-decline pattern (Figure S12), suggesting that biological uptake is not responsible for the observed remarkable decline of DIP. Thus, the observed DIP loss is ascribed to its resorption onto dust particles. There is no decline phase in the P release kinetics in seawater,[35,36,64] likely because resorption of DIP is disfavored in alkaline seawater.

Both dissolution of apatite (Ca−P) and desorption of surface weakly adsorbed P contribute to P release whereas P sorption reduces it. The observed DIP kinetics are the net results of the above three processes. The presence of a maximum in the DIP concentration suggests that the first two processes are faster than the resorption. A low pH favors apatite dissolution.[65] P sorption typically decreases with increasing pH due to lower positive surface charge of particles, and conversely, desorption is favorable at higher pH.[66] Thus, dust with various P speciation and mineralogy has different release behaviors in response to pH changes. Dust GM, McClP, and SASP all have higher DIP at pH 5 (Figure 6b−d) than at higher pHs (6.5 and 7.5), suggesting that the DIP release is controlled by dissolution of Ca−P. In contrast, dust REP shows the lowest DIP at pH 5 (Figure 6a), suggesting that P release is dominated by disfavored desorption of surface-labile P and/or favored resorption of DIP at low pH. The unique pH dependence of P release of REP can be ascribed to the much higher content of poorly crystalline Fe oxides (Table S2) favoring P resorption at lower pH, and/or the lower solubility of Ca−P in REP than in GM and SASP (Table 1). In addition, REP has a lower degree of P saturation ($DPS_{OX} = \frac{100[P]_{oxalate}}{[Fe + Al]_{oxalate}}$)[67] (17.2) than GM, McClP, and SASP (24.4, 31.5, and 25.9, respectively) (Table S4). $DPS_{OX}$ is a ratio of sorbed P to the P sorption capacity of dust based on oxalate extraction. The lower $DPS_{OX}$ value suggests the poorly crystalline Fe oxides in REP are less saturated with P adsorption or have more available sites for P adsorption, than those in the other three samples, consistent with the stronger resorption of P for REP. Thus, $DPS_{OX}$ can be used as an index to predict the potential of resorption of P back to the dust particles in lake water.

The solid residue of SASP after a 24-d release experiment at pH 6.5 was characterized by XANES spectroscopy. The lower shoulder peak indicates less Ca−P in the residue (Figure S14). Consistently, the Ca−P fraction decreases from 65.7% to 45.9% with an accompanying increase of the Fe−P fraction from 26.8% to 42.5% (Table S5). This result indicates resorption of P released from dissolution of Ca−P onto Fe oxides within the dust to form additional Fe−P. If the additional Fe−P did not form, then the dissolution of Ca−P alone would release about 20% (65.7−45.9% ≈ 20%) of TP, contradictory to the observed 2.1% release (Figure S13b). The redistribution of P species toward higher Fe−P fractions during acidic leaching is expected because the dust contains abundant Fe oxides (Table S2). This evidence strongly proves that the decline phase of the P release kinetics is due to the resorption of P back to the dust particles. This finding also provides support for the changes of P speciation in the dust by snowmelt processing prior to dust collection.

On the basis of per gram of dust particles, the amount of water-soluble P (16-h extraction) released in SEDEX is close to that released at the end of the leaching experiments at pH 6.5 and 7.5 but lower than that at pH 5 for GM, McClP, and SASP (Figure S13a). However, REP shows a lower release of P at both pH 5 and 7.5 than at pH 6.5 where the release is similar to the water-soluble P (Figure S13a). This result suggests that water-soluble P measured using deionized water in SEDEX cannot correctly assess the short-term availability of dust-borne P in acidified lakes from the perspectives of both the kinetics and the quantity of the P release.

**Environmental Implications.** Mineral dust is a significant source of P to the oligotrophic lakes of the central Rocky Mountains that have varying degrees of acidification.[39] Most such dust discussed here was generated from source areas within the western U.S. and particularly from basins on the Colorado Plateau on the basis of dust particle sizes, back-trajectory analyses, and direct observation (SI-1). The dominant Ca−P in the aeolian dust deposited to the lakes will be eventually dissolved by the acidic lake water and


DOI: 10.1021/acs.est.7b04729
Environ. Sci. Technol. 2018, 52, 2658−2667

transformed to either soluble P or P associated with Fe and Al oxides. However, the Ca−P species will likely remain in the sediments for lakes with circumneutral or alkaline pH. Therefore, the efficiency of dust deposition as P fertilizer depends strongly on lake water pH. The ongoing acidification of the alpine lakes in Colorado[68] will further promote dissolution of apatite and the related release of DIP and subsequent fixation by Fe and Al oxides as well, over decades or longer time periods.[69,70] However, a recovery from acidification[5] can impose opposite effects.

In the short term, water-soluble P is the major source of bioavailable P from dust after deposition into lakes. On the basis of the water-soluble portion (11.5−50.9 mg/L) and dust deposition rates in the southwestern U.S. (average 3.34 g $m^{-2}$ $a^{-1}$),[7] we can estimate that dust provides 38−170 $\mu$g $m^{-2}$ $a^{-1}$ DIP to lakes. Such values are likely underestimated for those lakes that have already been acidified because 1.3−2.7 times more DIP could be released at pH 5 than the so-called water-soluble P for most of the dust samples tested (Figure S13a). The temporal P release within a short-term after deposition is also critical to P availability. Phytoplankton can quickly incorporate DIP released from dust because the phosphate turnover time is 1−5 h in the oligotrophic surface water.[71,72] Such biologic uptake is faster than or comparable to our observed DIP release kinetics (Figure 6). Thus, the impact on lake ecosystems could be larger than indicated by the water-soluble P because 2 to 6 times more DIP than water-soluble P can be released when reaching the maxima (Figure 6).

However, we should be cautious about predicting the effects of lake acidification on the availability of dust-borne P. The presence of poorly crystalline Fe (and/or Al) oxides in the dust, dissolved Al in lake water, and Fe and Al oxides in overlying sediments all can scavenge more DIP released from enhanced apatite dissolution at lower pH.[5] The Fe and Al oxides in the dust with low $DPS_{OX}$ may even adsorb and remove the DIP originally present in the lakes. These processes would, however, decrease dust-borne P availability in the lakes.[73]

## ■ ASSOCIATED CONTENT

### Supporting Information

The Supporting Information is available free of charge on the ACS Publications website at DOI: 10.1021/acs.est.7b04729.

Details of the sampling sites, sample mineralogy, the Ca concentration and oxalate- and dithionite-extracted Al/Fe, dust back trajectories, particle size distribution, a satellite image of dust plumes, the SEDEX scheme, P reference compounds for XANES analyses, P K-edge XANES spectra for source sediments, correlations between P species and elevation, frequency histograms of P speciation between SEDEX and XANES results, DIP released during leaching experiments at 4 °C, $DPS_{ox}$, XANES LCF results of the 24-d leaching residue, and a comparison of DIP released and water-soluble P (PDF)

## ■ AUTHOR INFORMATION


### Corresponding Author

*Phone: 307-766-5523; E-mail: mzhu6@uwyo.edu (M.Z.).

### ORCID

Mengqiang Zhu: 0000-0003-1739-1055


### Notes

The authors declare no competing financial interest.

## ■ ACKNOWLEDGMENTS

This work was supported by Roy J. Shlemon Center for Quaternary Studies and the Wyoming Agricultural Experiment Station Competitive Grants Program at the University of Wyoming. Z.Z. is also thankful for the support from the Chinese Scholarship Council. We thank Chris Landry (Colorado Snow and Avalanche Center, Silverton) for collecting dust samples on snow. We are grateful to Ruth Heindel for her comments that improved this manuscript. This research was supported in part by the Climate and Land Use Change Program of the U.S. Geological Survey. Any use of trade, product, or firm names in this article is for descriptive purposes only and does not imply endorsement by the U.S. Government. The Canadian Light Source is supported by the Natural Sciences and Engineering Research Council of Canada, the National Research Council Canada, the Canadian Institutes of Health Research, the Province of Saskatchewan, Western Economic Diversification Canada, and the University of Saskatchewan.

## ■ REFERENCES


(1) Drever, J. I.; Zobrist, J. Chemical weathering of silicate rocks as a function of elevation in the southern Swiss Alps. *Geochim. Cosmochim. Acta* **1992**, *56* (8), 3209−3216.

(2) Müller, B.; Lotter, A. F.; Sturm, M.; Ammann, A. Influence of catchment quality and altitude on the water and sediment composition of 68 small lakes in Central Europe. *Aquat. Sci.* **1998**, *60* (4), 316−337.

(3) Sickman, J. O.; Melack, J. M.; Clow, D. W. Evidence for nutrient enrichment of high-elevation lakes in the Sierra Nevada, California. *Limnol. Oceanogr.* **2003**, *48* (5), 1885−1892.

(4) Jassby, A. D.; Reuter, J. E.; Axler, R. P.; Goldman, C. R.; Hackley, S. H. Atmospheric deposition of nitrogen and phosphorus in the annual nutrient load of Lake Tahoe (California-Nevada). *Water Resour. Res.* **1994**, *30* (7), 2207−2216.

(5) Kopáček, J.; Hejzlar, J.; Kaňa, J.; Norton, S. A.; Stuchlík, E. Effects of acidic deposition on in-lake phosphorus availability: a lesson from lakes recovering from acidification. *Environ. Sci. Technol.* **2015**, *49* (5), 2895−2903.

(6) Neff, J. C.; Ballantyne, A. P.; Farmer, G. L.; Mahowald, N. M.; Conroy, J. L.; Landry, C. C.; Overpeck, J. T.; Painter, T. H.; Lawrence, C. R.; Reynolds, R. L. Increasing eolian dust deposition in the western United States linked to human activity. *Nat. Geosci.* **2008**, *1* (3), 189−195.

(7) Brahney, J.; Ballantyne, A.; Kociolek, P.; Spaulding, S.; Otu, M.; Porwoll, T.; Neff, J. Dust mediated transfer of phosphorus to alpine lake ecosystems of the Wind River Range, Wyoming, USA. *Biogeochemistry* **2014**, *120* (1−3), 259−278.

(8) Brahney, J.; Mahowald, N.; Ward, D. S.; Ballantyne, A. P.; Neff, J. C. Is atmospheric phosphorus pollution altering global alpine Lake stoichiometry? *Glob. Biogeochem. Cycle* **2015**, *29* (9), 1369−1383.

(9) Tipping, E.; Benham, S.; Boyle, J.; Crow, P.; Davies, J.; Fischer, U.; Guyatt, H.; Helliwell, R.; Jackson-Blake, L.; Lawlor, A. J. Atmospheric deposition of phosphorus to land and freshwater. *Environ. Sci.: Processes Impacts* **2014**, *16* (7), 1608−1617.

(10) Mladenov, N.; Williams, M. W.; Schmidt, S. K.; Cawley, K. Atmospheric deposition as a source of carbon and nutrients to an alpine catchment of the Colorado Rocky Mountains. *Biogeosciences* **2012**, *9* (8), 3337−3355.

(11) Okin, G. S.; Mahowald, N.; Chadwick, O. A.; Artaxo, P. Impact of desert dust on the biogeochemistry of phosphorus in terrestrial ecosystems. *Glob. Biogeochem. Cycle* **2004**, *18* (2), GB2005.

(12) Camarero, L.; Catalan, J. Atmospheric phosphorus deposition may cause lakes to revert from phosphorus limitation back to nitrogen limitation. *Nat. Commun.* **2012**, *3* (1), 1118.

(13) Elser, J. J.; Andersen, T.; Baron, J. S.; Bergström, A.-K.; Jansson, M.; Kyle, M.; Nydick, K. R.; Steger, L.; Hessen, D. O. Shifts in lake N:




DOI: 10.1021/acs.est.7b04729
Environ. Sci. Technol. 2018, 52, 2658−2667

P stoichiometry and nutrient limitation driven by atmospheric nitrogen deposition. *Science* **2009**, *326* (5954), 835−837.
(14) Pulido-Villena, E.; Reche, I.; Morales-Baquero, R. Evidence of an atmospheric forcing on bacterioplankton and phytoplankton dynamics in a high mountain lake. *Aquat. Sci.* **2008**, *70* (1), 1−9.
(15) Morales-Baquero, R.; Pulido-Villena, E.; Reche, I. Atmospheric inputs of phosphorus and nitrogen to the southwest Mediterranean region: Biogeochemical responses of high mountain lakes. *Limnol. Oceanogr.* **2006**, *51* (2), 830−837.
(16) Ballantyne, A. P.; Brahney, J.; Fernandez, D.; Lawrence, C.; Saros, J.; Neff, J. C. Biogeochemical response of alpine lakes to a recent increase in dust deposition in the Southwestern, US. *Biogeosciences* **2011**, *8*, 2689.
(17) Chen, H.-Y.; Fang, T.-H.; Preston, M. R.; Lin, S. Characterization of phosphorus in the aerosol of a coastal atmosphere: Using a sequential extraction method. *Atmos. Environ.* **2006**, *40* (2), 279−289.
(18) Anderson, L.; Faul, K.; Paytan, A. Phosphorus associations in aerosols: What can they tell us about P bioavailability? *Mar. Chem.* **2010**, *120* (1), 44−56.
(19) Vicars, W. C.; Sickman, J. O.; Ziemann, P. J. Atmospheric phosphorus deposition at a montane site: Size distribution, effects of wildfire, and ecological implications. *Atmos. Environ.* **2010**, *44* (24), 2813−2821.
(20) Kar, G.; Hundal, L. S.; Schoenau, J. J.; Peak, D. Direct chemical speciation of P in sequential chemical extraction residues using P K-edge X-ray absorption near-edge structure spectroscopy. *Soil Sci.* **2011**, *176* (11), 589−595.
(21) Negassa, W.; Leinweber, P. How does the Hedley sequential phosphorus fractionation reflect impacts of land use and management on soil phosphorus: a review. *J. Plant Nutr. Soil Sci.* **2009**, *172* (3), 305−325.
(22) Prietzel, J.; Dumig, A.; Wu, Y. H.; Zhou, J.; Klysubun, W. Synchrotron-based P K-edge XANES spectroscopy reveals rapid changes of phosphorus speciation in the topsoil of two glacier foreland chronosequences. *Geochim. Cosmochim. Acta* **2013**, *108*, 154−171.
(23) Beauchemin, S.; Hesterberg, D.; Chou, J.; Beauchemin, M.; Simard, R. R.; Sayers, D. E. Speciation of phosphorus in phosphorus-enriched agricultural soils using X-ray absorption near-edge structure spectroscopy and chemical fractionation. *J. Environ. Qual.* **2003**, *32* (5), 1809−1819.
(24) Hesterberg, D.; Zhou, W. Q.; Hutchison, K. J.; Beauchemin, S.; Sayers, D. E. XAFS study of adsorbed and mineral forms of phosphate. *J. Synchrotron Radiat.* **1999**, *6*, 636−638.
(25) Sato, S.; Solomon, D.; Hyland, C.; Ketterings, Q. M.; Lehmann, J. Phosphorus speciation in manure and manure-amended soils using XANES spectroscopy. *Environ. Sci. Technol.* **2005**, *39* (19), 7485−7491.
(26) Ingall, E. D.; Brandes, J. A.; Diaz, J. M.; de Jonge, M. D.; Paterson, D.; McNulty, I.; Elliott, W. C.; Northrup, P. Phosphorus K-edge XANES spectroscopy of mineral standards. *J. Synchrotron Radiat.* **2011**, *18*, 189−197.
(27) Kraal, P.; Bostick, B. C.; Behrends, T.; Reichart, G.-J.; Slomp, C. P. Characterization of phosphorus species in sediments from the Arabian Sea oxygen minimum zone: Combining sequential extractions and X-ray spectroscopy. *Mar. Chem.* **2015**, *168*, 1−8.
(28) Longo, A. F.; Ingall, E. D.; Diaz, J. M.; Oakes, M.; King, L. E.; Nenes, A.; Mihalopoulos, N.; Violaki, K.; Avila, A.; Benitez-Nelson, C. R. P-NEXFS analysis of aerosol phosphorus delivered to the Mediterranean Sea. *Geophys. Res. Lett.* **2014**, *41* (11), 4043−4049.
(29) Hudson-Edwards, K. A.; Bristow, C. S.; Cibin, G.; Mason, G.; Peacock, C. L. Solid-phase phosphorus speciation in Saharan Bodélé Depression dusts and source sediments. *Chem. Geol.* **2014**, *384*, 16−26.
(30) Shen, Z.; Cao, J.; Arimoto, R.; Zhang, R.; Jie, D.; Liu, S.; Zhu, C. Chemical composition and source characterization of spring aerosol over Horqin sand land in northeastern China. *J. Geophys. Res.* **2007**, *112*, (D14).10.1029/2006JD007991
(31) Nenes, A.; Krom, M. D.; Mihalopoulos, N.; Van Cappellen, P.; Shi, Z.; Bougiatioti, A.; Zarmpas, P.; Herut, B. Atmospheric acidification of mineral aerosols: a source of bioavailable phosphorus for the oceans. *Atmos. Chem. Phys.* **2011**, *11* (13), 6265−6272.
(32) Stockdale, A.; Krom, M. D.; Mortimer, R. J. G.; Benning, L. G.; Carslaw, K. S.; Herbert, R. J.; Shi, Z.; Myriokefalitakis, S.; Kanakidou, M.; Nenes, A. Understanding the nature of atmospheric acid processing of mineral dusts in supplying bioavailable phosphorus to the oceans. *Proc. Natl. Acad. Sci. U. S. A.* **2016**, *113* (51), 14639−14644.
(33) Abouchami, W.; Näthe, K.; Kumar, A.; Galer, S. J. G.; Jochum, K. P.; Williams, E.; Horbe, A. M. C.; Rosa, J. W. C.; Balsam, W.; Adams, D.; Mezger, K.; Andreae, M. O. Geochemical and isotopic characterization of the Bodélé Depression dust source and implications for transatlantic dust transport to the Amazon Basin. *Earth Planet. Sci. Lett.* **2013**, *380*, 112−123.
(34) de Negreiros, G. H.; Nepstad, D. C. Mapping deeply rooting forests of Brazilian Amazonia with GIS. *Proc. ISPRS Comm. VII Symp. - Resour. Environ. Monit.* **1994**, 334−338.
(35) Ridame, C.; Guieu, C. Saharan input of phosphate to the oligotrophic water of the open western Mediterranean Sea. *Limnol. Oceanogr.* **2002**, *47* (3), 856−869.
(36) Mackey, K. R. M.; Roberts, K.; Lomas, M. W.; Saito, M. A.; Post, A. F.; Paytan, A. Enhanced solubility and ecological impact of atmospheric phosphorus deposition upon extended seawater exposure. *Environ. Sci. Technol.* **2012**, *46* (19), 10438−10446.
(37) Louis, J.; Bressac, M.; Pedrotti, M. L.; Guieu, C. Dissolved inorganic nitrogen and phosphorus dynamics in seawater following an artificial Saharan dust deposition event. *Front. Mar. Sci.* **2015**, *2*, 27.
(38) Baron, J.; McKnight, D.; Denning, A. S. Sources of dissolved and particulate organic material in Loch Vale Watershed, Rocky Mountain National Park, Colorado, USA. *Biogeochemistry* **1991**, *15* (2), 89−110.
(39) Musselman, R. C.; Slauson, W. L. Water chemistry of high elevation Colorado wilderness lakes. *Biogeochemistry* **2004**, *71* (3), 387−414.
(40) Mast, M. A.; Turk, J. T.; Clow, D. W.; Campbell, D. H. Response of lake chemistry to changes in atmospheric deposition and climate in three high-elevation wilderness areas of Colorado. *Biogeochemistry* **2011**, *103* (1−3), 27−43.
(41) Reynolds, R. L.; Munson, S. M.; Fernandez, D.; Goldstein, H. L.; Neff, J. C. Concentrations of mineral aerosol from desert to plains across the central Rocky Mountains, western United States. *Aeolian Res.* **2016**, *23*, 21−35.
(42) Neff, J. C.; Reynolds, R. L.; Munson, S. M.; Fernandez, D.; Belnap, J. The role of dust storms in total atmospheric particle concentrations at two sites in the western US. *J. Geophys. Res. Atmos.* **2013**, *118* (19), 11201−11212.
(43) Skiles, S. M.; Painter, T. H.; Belnap, J.; Holland, L.; Reynolds, R. L.; Goldstein, H. L.; Lin, J. Regional variability in dust-on-snow processes and impacts in the Upper Colorado River Basin. *Hydrol. Processes* **2015**, *29* (26), 5397−5413.
(44) Aarons, S. M.; Blakowski, M. A.; Aciego, S. M.; Stevenson, E. I.; Sims, K. W.; Scott, S. R.; Aarons, C. Geochemical characterization of critical dust source regions in the American West. *Geochim. Cosmochim. Acta* **2017**, *215*, 141−161.
(45) McCave, I.; Manighetti, B.; Robinson, S. Sortable silt and fine sediment size/composition slicing: parameters for palaeocurrent speed and palaeoceanography. *Paleoceanography* **1995**, *10* (3), 593−610.
(46) Ross, G.; Wang, C. Extractable Al, Fe, Mn, and Si. In *Soil Sampling and Methods of Analysis*; Carter, M. R., Ed.; CRC Press: Boca Raton, FL, 1993; pp 239−246.
(47) Ruttenberg, K. C. Development of a sequential extraction method for different forms of phosphorus in marine sediments. *Limnol. Oceanogr.* **1992**, *37* (7), 1460−1482.
(48) Berner, R. A.; Rao, J.-L. Phosphorus in sediments of the Amazon River and estuary: Implications for the global flux of phosphorus to the sea. *Geochim. Cosmochim. Acta* **1994**, *58* (10), 2333−2339.
(49) Koroleff, F. Determination of phosphorus. In *Methods for Seawater Analysis*; Grasshoff, K., Ehrhardt, M., Kremling, F., Eds.; Wiley: New York, 1983; pp 125−139.


DOI: 10.1021/acs.est.7b04729
*Environ. Sci. Technol.* 2018, 52, 2658−2667

(50) Anagnostou, E.; Sherrell, R. M. MAGIC method for subnanomolar orthophosphate determination in freshwater. *Limnol. Oceanogr.: Methods* **2008**, *6* (1), 64−74.
(51) Clow, D. W.; Ingersoll, G. P. Particulate carbonate matter in snow from selected sites in the south-central Rocky Mountains. *Atmos. Environ.* **1994**, *28* (4), 575−584.
(52) Reynolds, R.; Belnap, J.; Reheis, M.; Lamothe, P.; Luiszer, F. Aeolian dust in Colorado Plateau soils: nutrient inputs and recent change in source. *Proc. Natl. Acad. Sci. U. S. A.* **2001**, *98* (13), 7123−7127.
(53) Rhoades, C.; Elder, K.; Greene, E. The influence of an extensive dust event on snow chemistry in the Southern Rocky Mountains. *Arct. Antarct. Alp. Res.* **2010**, *42* (1), 98−105.
(54) Artaxo, P.; Martins, J. V.; Yamasoe, M. A.; Procópio, A. S.; Pauliquevis, T. M.; Andreae, M. O.; Guyon, P.; Gatti, L. V.; Leal, A. M. C. Physical and chemical properties of aerosols in the wet and dry seasons in Rondônia, Amazonia. *J. Geophys. Res.* **2002**, *107* (D20), 8081−8095.
(55) Benitez-Nelson, C. R. The biogeochemical cycling of phosphorus in marine systems. *Earth-Sci. Rev.* **2000**, *51* (1−4), 109−135.
(56) Ensslin, A.; Rutten, G.; Pommer, U.; Zimmermann, R.; Hemp, A.; Fischer, M. Effects of elevation and land use on the biomass of trees, shrubs and herbs at Mount Kilimanjaro. *Ecosphere* **2015**, *6* (3), 1−15.
(57) Flaum, J. A. Investigation of phosphorus cycle dynamics associated with organic carbon burial in modern (North Pacific) and ancient (Devonian and Cretaceous) marine systems: Strengths and limitations of sequentially extracted (SEDEX) phosphorus data. Ph.D. Dissertation, Northwestern University, Evanston, IL, p 196., 2008.
(58) Guo, B.; Yang, H.; Li, Y. The speciation of phosphorus in the sand particles in western Inner Mongolia. *Proceedings of Second International Conference on Mechanic Automation and Control Engineering (MACE)*; IEEE: 2011; pp 2755−2757.
(59) Baker, A. R.; Jickells, T. D.; Witt, M.; Linge, K. L. Trends in the solubility of iron, aluminium, manganese and phosphorus in aerosol collected over the Atlantic Ocean. *Mar. Chem.* **2006**, *98* (1), 43−58.
(60) Ajiboye, B.; Akinremi, O. O.; Jürgensen, A. Experimental validation of quantitative XANES analysis for phosphorus speciation. *Soil Sci. Soc. Am. J.* **2007**, *71* (4), 1288−1291.
(61) Claff, S. R.; Sullivan, L. A.; Burton, E. D.; Bush, R. T. A sequential extraction procedure for acid sulfate soils: partitioning of iron. *Geoderma* **2010**, *155* (3), 224−230.
(62) Pomeroy, L. R.; Wiebe, W. J. Energetics of microbial food webs. *Hydrobiologia* **1988**, *159* (1), 7−18.
(63) Rivkin, R. B.; Anderson, M.; Lajzerowicz, C. Microbial processes in cold oceans. I. Relationship between temperature and bacterial growth rate. *Aquat. Microb. Ecol.* **1996**, *10* (3), 243−254.
(64) Ridame, C.; Moutin, T.; Guieu, C. Does phosphate adsorption onto Saharan dust explain the unusual N/P ratio in the Mediterranean Sea? *Oceanol. Acta* **2003**, *26* (5), 629−634.
(65) Andersson, K. O.; Tighe, M. K.; Guppy, C. N.; Milham, P. J.; McLaren, T. I.; Schefe, C. R.; Lombi, E. XANES demonstrates the release of calcium phosphates from alkaline vertisols to moderately acidified solution. *Environ. Sci. Technol.* **2016**, *50* (8), 4229−4237.
(66) Haynes, R. J. Effects of liming on phosphate availability in acid soils. *Plant Soil* **1982**, *68* (3), 289−308.
(67) Hooda, P.; Rendell, A.; Edwards, A.; Withers, P.; Aitken, M.; Truesdale, V. Relating soil phosphorus indices to potential phosphorus release to water. *J. Environ. Qual.* **2000**, *29* (4), 1166−1171.
(68) Bowman, W. D.; Murgel, J.; Blett, T.; Porter, E. Nitrogen critical loads for alpine vegetation and soils in Rocky Mountain National Park. *J. Environ. Manage.* **2012**, *103*, 165−171.
(69) Golterman, H.; Paing, J.; Serrano, L.; Gomez, E. Presence of and phosphate release from polyphosphates or phytate phosphate in lake sediments. *Hydrobiologia* **1997**, *364* (1), 99−104.
(70) Stoddard, J. L.; Van Sickle, J.; Herlihy, A. T.; Brahney, J.; Paulsen, S.; Peck, D. V.; Mitchell, R.; Pollard, A. I. Continental-scale increase in lake and stream phosphorus: are oligotrophic systems disappearing in the United States? *Environ. Sci. Technol.* **2016**, *50* (7), 3409−3415.
(71) Xu, J.; Yin, K.; Ho, A. Y.; Lee, J. H.; Anderson, D. M.; Harrison, P. J. Nutrient limitation in Hong Kong waters inferred from comparison of nutrient ratios, bioassays and 33P turnover times. *Mar. Ecol.: Prog. Ser.* **2009**, *388*, 81−97.
(72) Moutin, T.; Thingstad, T. F.; Van Wambeke, F.; Marie, D.; Slawyk, G.; Raimbault, P.; Claustre, H. Does competition for nanomolar phosphate supply explain the predominance of the cyanobacterium Synechococcus? *Limnol. Oceanogr.* **2002**, *47* (5), 1562−1567.
(73) Akhurst, D.; Jones, G. B.; McConchie, D. M. The application of sediment capping agents on phosphorus speciation and mobility in a sub-tropical dunal lake. *Mar. Freshwater Res.* **2004**, *55* (7), 715−725.

## NOTE ADDED AFTER ASAP PUBLICATION

This article published with incorrect versions of the TOC and Figure 3 files. The corrected versions published February 21, 2018.


DOI: 10.1021/acs.est.7b04729
*Environ. Sci. Technol.* 2018, 52, 2658−2667